UW Journal of Science and Technology Vol. 6 (2022) 19-25
ISSN: 2523-0123 (Print) 2616-4396 (Online)

University of Wah
Journal of Science and Technology

www.uow.edu.pk

Video Based Automatic White Blood Cell Tracking by Improving Centroid Coordinates

Huma Hafeez and Ch Asad Abbas

***Abstract*— The study of blood flow physiognomies, cellular illnesses, lesion vasculature, and brain micro blood vessels is influenced by white blood cell tracking, velocity measures and the white blood cell (WBC) mechanism to overwhelm the bacteria. We have demonstrated an improvement in the accuracy of centroid tracking algorithm which identifies each probe particle with different threshold intensity in one source frame. Centroid tracking algorithm facilitates to recognize, locate and track particles simultaneously from the first to the end for a series of frames. In the current work, a microscopic video in which WBC attacking a small bacterium is used. The proposed tracking system mainly consists of detecting and localizing WBCs in given frame within the video via blob analysis. Automatic ROI (region of interest) detection is accomplished by recognizing the suitable connected component number that fulfils the complete segregation between WBC and harmful bacteria. This separation is achieved by removing little items with pixel values less than P pixels. Because the WBC centroid and bacteria were so close in some frames, the proposed green star marker was employed to fine-tune the tracking procedure. The whole process took 0.03 seconds to complete one iteration which makes it highly time efficient.**

***Index Terms*— Microscopic object detection, microscopic object tracking, Dilation, Blob analysis, Centroid based tracking.**

Nomenclature:

WBC	White Blood Cells
ROI	Region of Interest
RGB	Red, green and blue
GSBC	Green star based centroid
FPS	Frames per second

Manuscript received: Apr 15, 2022; accepted: Oct 4, 2022

H. Hafeez (email:huma.asad918@yahoo.com) is affiliated with School of Mechanical Engineering, Shandong University, Jinan, China.

C. A. Abbas (email: chasad573@yahoo.com) is affiliated with the Department of Mechatronics Engineering, University of Chakwal, Pakistan.

*Corresponding author email:huma.asad918@yahoo.com

I. Introduction

As the tracking process reflects the features of blood cells and defines a variety of diseases, the automated blood cells tracking system plays an important function. Due of the fragile nature of blood cells, variances in their sizes, and the presence of various moving chemicals going through the blood, blood cell monitoring is difficult.

White blood cells tracking, and velocity measurements are active research areas that influence the study of blood flow physiognomies, cellular diseases, lesion vasculature, cerebral micro blood vessels, and the white blood cell (WBC) mechanism to overwhelm the bacteria [1]. The study of WBC symptoms and movements outside of non-functional areas of cultural processing allows for a quick diagnosis and accurate investigation of WBC symptoms and movements. WBC detection from body fluid is required for such a surveillance system, which is a complex and difficult operation. Video microscopic processing is critical in cell biology for quantitatively studying the cell motion trajectory [2]. When the body is attacked by an illness or disease, the immune system usually responds by activating more leukocytes [3]. As a result, counting the number of these cells is a reasonably simple technique to detect and track such circumstances.

Many traditional tracking methods (such as mean shift algorithm, kalman filter) have been developed, they have low computational cost but are unable to recognize the entire object due to frame differences [4]. Zhou et al. [5] suggested an optical flow approach for detecting moving objects when the camera is moving. It did, however, take longer to detect the moving object. Although Mean Shift Tracking algorithm [6] can track objects in real time, it has a high level of complexity when it comes to detecting many items. Because a single core takes longer to handle several objects, some frames are lost in real time. Eden et al. [7] used an artificial neural network to detect various blood cell types and constructed an automated cell tracking system to assess cells circulatory patterns and behavioral tendencies in vivo video. Xiao et al. [8] used the object color model histogram to represent the reference blood cell model. Without sacrificing generality, the blood cell model

can be considered centered at the spatial point. Singh et al. [9] developed an algorithm for real-time tracking of moving object using color feature and motion. They pre-processed the frame to convert it from RGB to grayscale as it takes less time in handling. Median filter was applied to eliminate clamor from frames of video. Object tracking was done on the basis of region properties i.e. centroid, bounding box etc. to eliminate noise and prevent edges, median filtering was considered as far better than convolution technique.

Rohr et al. [10] classified the tracking into two categories, i.e. tracking via model evaluation and tracking via detection. Mehta el al. [11] presented an approach to grab the video frame and track the object in real-time using static camera. For automated object tracking, they implemented the concept of frame subtraction and histogram matching. Discrete Kalman filter was implemented to determine the object position by using prediction equation and correction equation. Rapoport et al. [12] addressed the cell tracking problem in part by presenting a method for determining the accuracy of cell tracking results as well as a dataset containing two hand - labeled brightfield microscopy videos. Xiang et al. [13] reviewed the image representation, appearance model and motion model for tracking either single or multiple targets. They found that fragment based object representation was robust in case of occlusions and background noise, weakly supervised online manner recovers the error, optical flow based motion estimator may cause mismatches with illumination change, particle filter tracker did not track accurately and deformable part models were accurate detectors.

Mohapatra et al. [14] proposed a method for tracking multi-moving bacteria and white blood cells using the Multi-threading parallel idea in a microscopic blood cell video (WBC). This method uses a continuously adaptive mean shift algorithm with a color model to track several moving bacteria using a multi-threading concept and comparing the mean of each frame in the movie. When the mean shift vector converges, it is possible to track bacteria in the next frame. To detect WBC velocity and sketch its course, a green star based centroid (GSBC) moving white blood cell (WBC) tracking technique was presented by Ata et al. [15]. The suggested cell tracking system has two stages: WBC detection and blob analysis, as well as fine-tuning the tracking process by identifying the centroid of the WBC and marking the centroid for finer tracking and eliminating bacteria from the bounding box, are the two steps of the recommended cell tracking system. The WBC motion's speed and trajectory are also measured and plotted. An optical flow technique is compared to the suggested tracking system in the experiments, demonstrating that the proposed system is superior because the optical flow method failed to track the WBC.

Our proposed tracking system mainly consists of converting the selected dataset from colored scale to greyscale to compensate the environmental effects. WBCs detection and localization in each frame within the video is accomplished via blob analysis. Automatic ROI detection is accomplished by recognizing the suitable connected component number that fulfils the complete segregation between WBC and harmful bacteria. This separation is achieved by removing little items with pixel values less than P pixels. Because the WBC centroid and bacteria were so close in some frames, the proposed green star marker was employed to fine-tune the tracking procedure.

II. PROPOSED METHODOLOGY

Our suggested methodology consists of dataset collection, basic image processing and morphological operations for WBC detection and then, centroid calculation is order to track respective WBC in each frame, respectively. Flow chart of proposed methodology is expressed in *Fig. 1.*

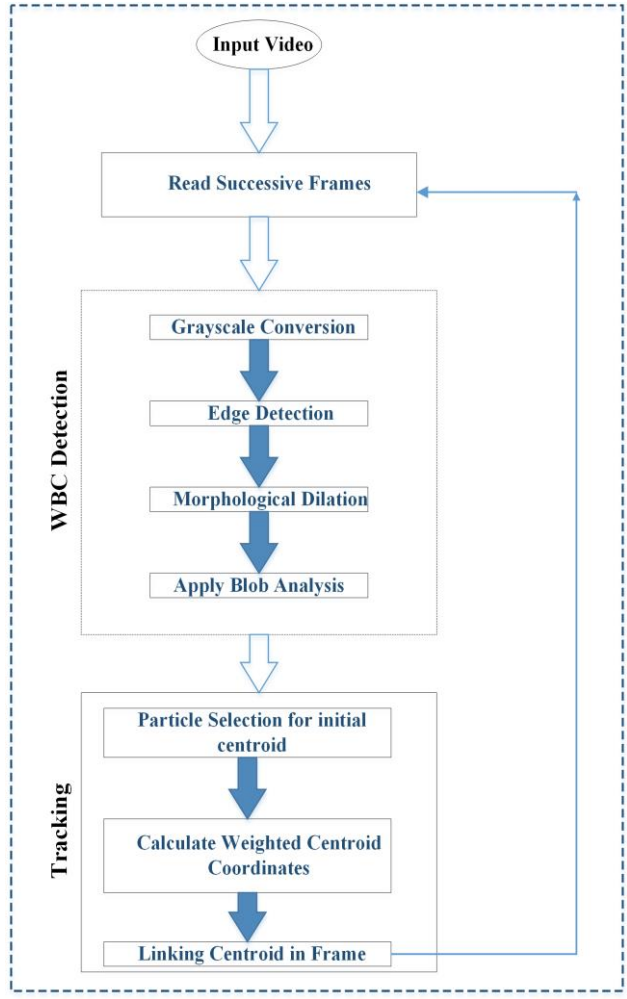

Fig. 1. Flow Chart for WBC detection and Tracking

A. Dataset Collection

A video dataset in which the white blood cell is chasing bacteria [15] is used in our work. The dataset consists of 28.4667 seconds video having 426 frames. Its frame rate is 15 FPS and 24 bits per pixel. Some of its sample frames are shown in *Fig.1.*

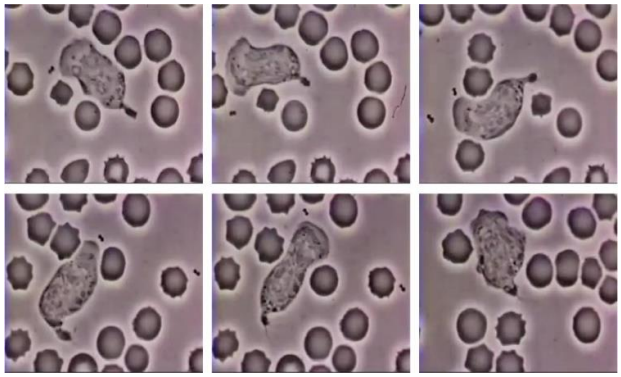

Fig. 2. Sample Frames of Dataset

B. Gray Scale conversion

To detect and track a white blood cell in a video, a colored experimental video is converted into a limited number of gray frames [16]. The effects of sudden environmental changes can be compensated by incorporating the mean of every frame in gray scale format. Working with a gray scale format reduces the need for calculation and memory time. So, we converted the whole dataset first into grayscale and then computed the mean of those grayscale frames and mean of their respective red, green and blue channels of grayscale frames. The mean intensities in gray levels are shown in *Fig. 2*.

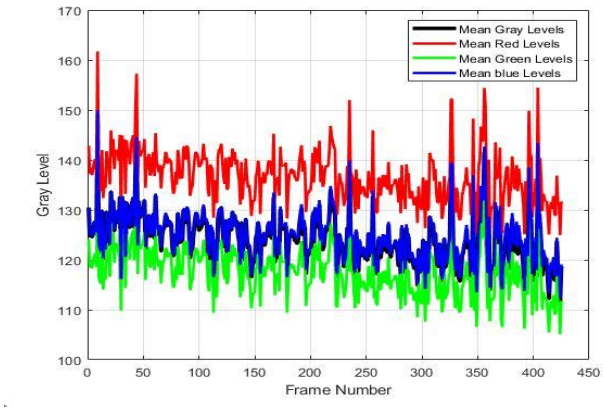

Fig. 3. Mean intensities of Gray levels

C. Edge Detection

To detect the edge correctly, canny edge detector [17] will be used. To detect the wide range of edges in an image, a multi-stage based canny edge detector algorithm is employed. In our case, it consists of following steps:

i. Gaussian Filter

After taking mean of gray level intensities of each frame, each frame is smoothed with Gaussian filter in order to lessen noise, unnecessary details and textures. A Gaussian filter [18] is used to cut out the noise and smooth the edges as the high frequency feature. This will increase the probability of losing the weak edges and consequently, the appearance of isolated edges. Using a properly designed Gaussian filter, we can be very certain about the range of spatial frequencies that remain visible in the image after filtering. It is computed by using the following expression [18]:

$$g(x,y) = G_\sigma(m,n) * f(x,y) \quad (1)$$

$$G_\sigma(m,n) = \frac{1}{\sqrt{2\pi\sigma}} exp(-\frac{m^2+n^2}{2\sigma^2}) \quad (2)$$

Where $G_\sigma(m,n)$ is the filter kernel function, m denotes the distance from the origin in the horizontal axis, the distance from the origin in the vertical axis is denoted by n, while the standard deviation of the Gaussian distribution is denoted by σ.

ii. Sobel Gradient

After smoothing the frame by Gaussian filter, we have computed appropriate gradient $g(x,y)$by using Sobel Gradient. Sobel operators are a combination of Gaussian smoothing and differentiation, making them more noise resistant. The Sobel operator is slower, but its larger convolution kernel smoothens the input image more thoroughly, making it less sensitive to noise. The obtained gradient approximations can be merged at each place in the image to give the gradient magnitude [19], using:

$$G(m,n) = \sqrt{{G_m}^2 + {G_n}^2} \quad (3)$$

Using this information, we can also calculate the gradient's direction. The spatial gradient is caused by the angle of orientation of the edge (relative to the pixel grid):

$$\vartheta = arctan\frac{G_n}{G_m} \quad (4)$$

where ϑ is 0 for a vertical edge which is lighter on the right side. In this situation, orientation 0 refers to the direction of highest contrast from black to white on the image, which runs from left to right, and all angles are measured anti-clockwise from there. The directional angle is turned in one of four angles (0 °, 45 °, 90 °, and 135 °) that represent vertical, horizontal, and two diagonals. On maps up to 0 °, the direction of the edge that falls in each color zone will be adjusted to the values of a specific angle, such as [0 °, 22.5 °] or [157.5 °, 180 °].

iii. Magnitude Thresholding

After Sobel filter, we have applied the thresholding on G to eliminate the background regions [20]. Thresholding is employed on grayscale filtered image to create binary images. After the grayscale image has appeared, it is thresholded. Gray values over the threshold are treated in the same way as white pixels. Some are black pixels. The threshold in our case will be:

$$G_T = \begin{cases} G(m,n)\ if G(m,n) > U \\ 0 \qquad otherwise \end{cases} \quad (5)$$

We will suppress the edges non-maxima pixels in $G_T$gained above the thin edge ridges which has broadened in Gaussian filter. To preserve $G_T$unchanged, it must be confirmed that the non-zero $G_T(m,n)$is bigger than its two neighbors along the gradient direction; otherwise, it will be set to 0. Next, previous result will be thresholded by the two different thresholds $T_{thresh1}$ and $T_{thresh2}$ so that $T_{thresh1} < T_{thresh2}$ to attain two binary images BW1 and BW2. Results with larger values of $T_{thresh2}$ will have less noise but greater gaps between edge segments.

If the value of the pixel gradient on the edge is greater than the maximum limit value, it is marked as a solid boundary pixel. It is recognized as a pixel on the weak edge if the value of the pixel gradient on the edge is less than the maximum limit value but larger than the lower limit value. If the value of the pixel gradient on the edge is less than the value of the lower limit, it will be compressed. Both boundary values are strongly determined, and their meaning will depend on the content of the input image provided. The follow-up framework for the acquisition of the Canny Edge detector is shown in *Fig. 3*.

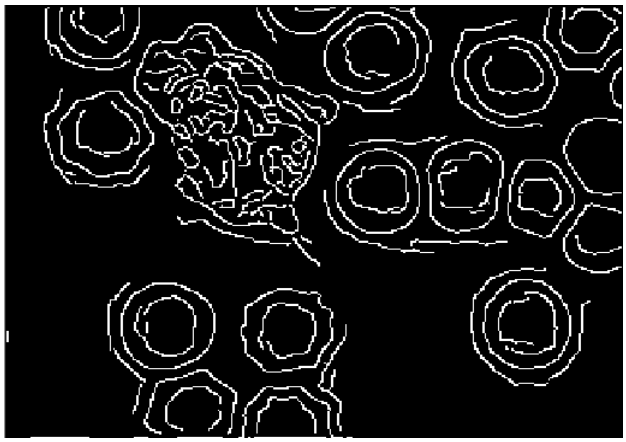

Fig. 4. Output of Canny edge detection

D. Dilation

After edge detection, dilation is done to adds pixels to the boundaries of objects in an image. The morphological dilation operation uses a structuring element to expands or thickens foreground objects in an image. The dilation operator takes two inputs, first one is needed to be dilated and second one consists of structuring element i.e. kernel consisting of set of coordinate points. It will determine the dilation precise effect at the input image. The mathematical expression for dilation performed on the binary images is as follows:

- Let M be the Euclidean coordinates set corresponding to the binary image as an input and N be the structuring element set of coordinates.
- Consider N_x representing the N translation and having its origin at x.
- After that dilating M by N consists of set of all points x so that the N_x intersection with M should be non-empty.

Consider BW2 as resultant image obtained after the canny edge detector implementation and S be the structuring element [19], the mathematics in dilation will include:

$$BW2 \oplus S = \{e \in E | (S^z)_e \cap BW1 \neq \varphi\} \quad (6)$$

Where S^z denotes the symmetric of S, which is:

$$S^z = \{s \epsilon E | -s \epsilon E\} \quad (7)$$

Where E be a Euclidean distance or an integer grid. Dilation output is shown in *Fig. 4*, for hole filling in dilated image, the flood-fill operation is implemented as expressed in Eq. 8.

$$L_h = (L_{h-1} \oplus S \cap BW1^c) \quad (8)$$

It will perform a flood-fill operation on binary images which will be useful in removing inappropriate artifacts from images. It converts linked background pixels (0s) to foreground pixels (1s) in binary images, pausing when it hits object borders. The output is shown in *Fig. 5*.

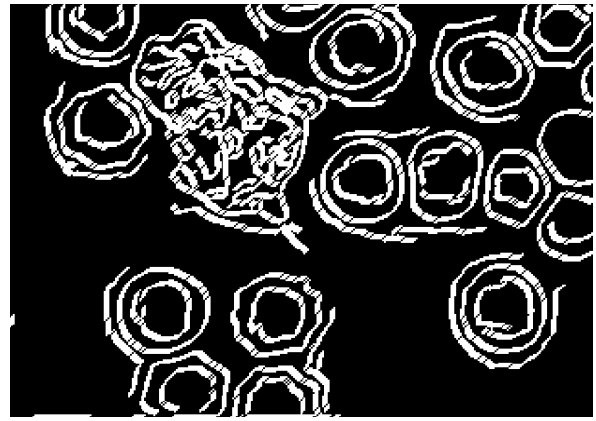

Fig. 5. Output of Morphological Dilation

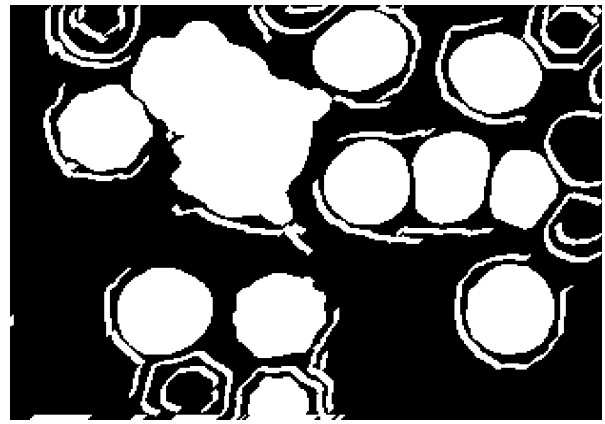

Fig. 6. Output of Flood-Fill operation

E. Blob Analysis

Blob analysis will be performed to remove the small objects having lesser pixel value than binary image in order to isolate the region containing WBCs. The blob detection algorithm [21] can detect all the available blobs in binary image. In our case, larger blobs will be accepted, as WBC is quite larger in size than RBC, while others will be rejected. It is not required to use a specific detection category if no blob is allowed, since the object detection method accommodates for the absence of an object. In case of acceptable blobs, for the precise tracking stage, the rectangular detected blobs are considered to be initial inputs. The first stage of the suggested WBC tracking system for blob extraction is termed the first stage, which is followed by the second stage in order to recognize the distinct blobs whether they are WBC or not. This recognition process consists of mainly two steps i.e. presenting each blob by specific features and using the same method to compare the features of each blob.

Typically, the bounding box of a blob i.e. the smallest rectangle containing the blob, is defined by moving across all the blob pixels and finding the four pixels. It uses the

state of art of blob detector centered on normalized Laplacian of Gaussian (LOG)norm [22] as:

$$L\,(x,y,t)\; =\; K(x,y,t)\; *\; I\,(x,y,t) \quad (9)$$

Where $K(x,y,t)$is the Gaussian kernel at a certain scale t to give a scale space representation given in Eq. 10 and $I(x,y,t)$ is the video frame.

$$K(x,y,t) = \frac{1}{2\pi t} e^{-\frac{x^2+y^2}{2t^2}} \qquad (10)$$

The resultant (LOG)norm can be estimated as:

$$\nabla^2_{norm} L = t(L_{xx} + L_{yy}) \qquad (11)$$

The setup of the blob analysis consists of extracting the region corresponding to the objects via thresholding techniques, filtering the extracted ROI via region transformation techniques. The blob detection and the extracted WBC for further tracking is shown in *Fig. 6*.

Fig. 7. Output of Blob Detection Analysis

F. Tracking Algorithm

The main purpose for the proposed method is to properly detect and monitor a quickly moving WBC when it is attacking a very small bacterium, and the WBC and the bacterium have a large size difference. So, a green star based centroid, to generate a masked video for next stage, tracking algorithm is proposed for WBC speed measurement. To ensure exact WBC localization, this green centroid was proposed. Furthermore, a fine-tuned tracking technique based on blob analysis is obtained in order to monitor the WBC in a video.

Automatic ROI detection is accomplished by recognizing the suitable connected component number that fulfils the complete segregation between WBC and harmful bacteria. This separation is achieved by removing little items with pixel values less than P. It is evident that when WBC begins to attack bacteria, they are affected by each other.

Centroid based algorithm [23] is used for tracking WBC in successive frames. Main steps in the proposed algorithm are:

Step 1) Selection of candidate particles and determination of the initial centroids

Step 2) Calculation of the weighted centroid coordinate of each candidate particle and

Step 3) Link the centroids in a series of frames into trajectories for each particle.

The cut off $I_{cut\text{-}off}$ was applied to each smoothed local image IS to obtain the local image I_L using Eq. 13:

$$I_L(u,v) = \begin{cases} I_s(u,v) & if\ I_s(u,v) > I_{cut-off} \\ 0 & otherwise \end{cases} \quad (12)$$

where $I_s(u,v)$ is the pixel intensity in the I_s indexed by integer u = 1, ..., ds as the pixel row index and v = 1, ..., ds as the pixel column index and $I_L(u,v)$is the pixel intensity of the I_LIn Eq. 15, pixel intensity greater than $I_{cut-off}$are unaltered while pixel intensity lower than $I_{cut-off}$ are set to zero. It is expected that the intensity weighted centroid could provide sub pixel resolution for the particle tracking

The speed of the WBC is calculated by locating the centroid in two consecutive frames in x and y directions, where Euclidean distance is computed via following expression:

$$Euclidean\ Distance = \sqrt{[x(i) - x(i-1)]^2 + [y(i) - y(i-1)]^2} \quad (13)$$

All of these centroids are stored in matrix A in order to calculate the median (M) of this matrix, respectively. The WBC speed is computed as:

$$Speed = M * \frac{Number\ of\ frames}{Video\ duration} \qquad (14)$$

III. EXPERIMENTAL RESULTS

Our algorithm is implemented on the system consisting of Windows 10 Pro, Intel® Core™ i5-6200U CPU @ 2.30GHz processor with 8GB RAM with MATLAB 2020b and is applied on the video sequence consisting of 426 frames. We have computed the centroid location in horizontal and vertical axis along with speed of WBC in each frame. The tracking of white blood cells using centroid in successive frames is shown in *Fig. 7*. It can be seen clearly that WBC is detected and tracked successful in respective frames.

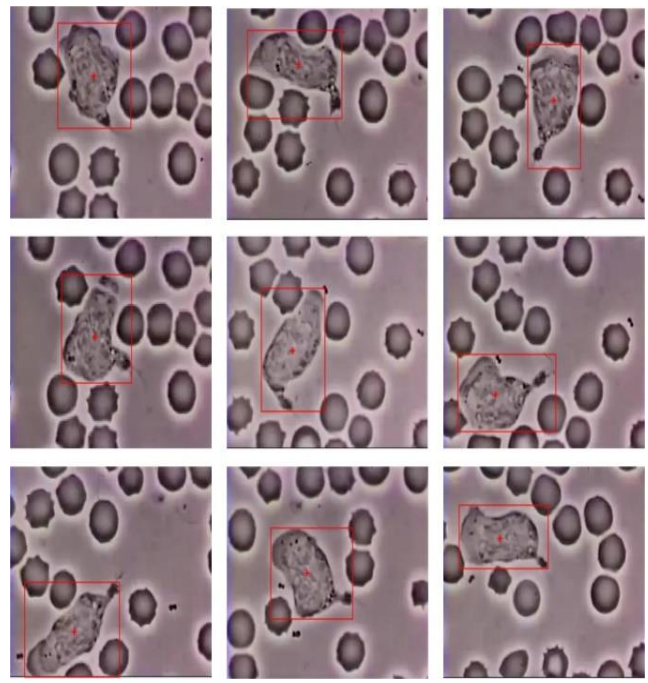

Fig. 8. Tracking of WBC in successive frames

Fig. 8, represents the speed of white blood cell in µm while attacking the small bacterium which is assessed as per time and Euclidean distance. Horizontal axis denotes the consecutive video frame number and the vertical axis denotes the speed per frame which is calculated by using centroid location co-ordinates.

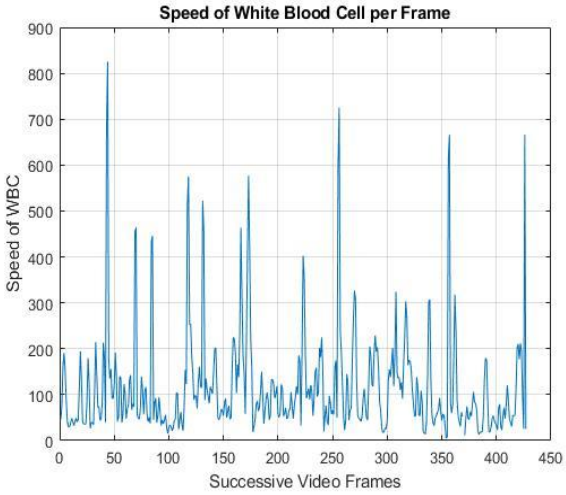

Fig. 9. Speed of WBC in successive frame

Some of the samples of centroid direction (degrees) is shown in Table 5.1. The whole process takes an average of 0.03 seconds to detect and track the WBC in each frame. So, it is highly efficient algorithm to track WBC.

TABLE 1
WBC'S CENTROID DIRECTION IN CORRESPONDING FRAME

Frame Number	Centroid Location in Horizontal Axis	Centroid Location in Vertical Axis
1	148.35	94.48
2	144.39	93.05
4	135.47	88.74
6	136.60	88.47
8	131.34	87.701
10	127.71	86.09
20	114.56	77.28
30	78.79	85.01
40	54.57	100.92
50	154.46	118.14
60	121.52	142.30
70	83.75	149.48
80	114.04	146.56
90	145.67	128.87
100	127.50	120.95
110	106.46	118.50
120	142.37	116.36
130	121.17	129.88
140	155.31	134.82
150	132.36	165.65
160	107.57	183.93
170	169.13	141.36
180	122.89	171.97
200	77.74	173.90
240	111.37	121.00
280	176.19	105.76
320	120.74	67.70
360	127.71	122.45
400	133.32	91.79
426	125.08	65.21

IV. CONCLUSION

The identification and monitoring of blood cells is essential for understanding how biological cells behave and function in various contexts. The video-microscopy for WBC attacking a microscopic bacterium is taken into consideration in the current work. The WBC detection stage of the suggested tracking system was in charge of locating the WBC utilizing blob analysis in a certain frame of the video. The centroid of the WBC is then marked with a proposed green star marker, excluding the bacteria because they are too close in some frames, to further fine-tune the tracking method. Additionally, the speed of the migrating WBC is depicted. The whole process took 0.03 seconds to complete one iteration which makes it highly time efficient.

REFERENCES

[1] L. Pelkmans, J. Kartenbeck, and A. Helenius, Caveolar endocytosis of simian virus 40 reveals a new two-step vesicular-transport pathway to the ER. Nature cell biology, Vol. 3(5), pp. 473-483, 2001.

[2] J. B. Dixon, D. C., Zawieja, A. A. Gashev, A. A., and G. L. Coté, Measuring microlymphatic flow using fast video microscopy. Journal of biomedical optics, Vol. 10(6), pp. 064016, 2005.

[3] L. B. Nicholson, The immune system. Essays Biochem, Vol. 60(3), pp. 275-301, 2016.

[4] V. K. Agarwal, N. Sivakumaran and V. P. S. Naidu, Six object tracking algorithms: A comparative study. Indian Journal of Science and Technology, Vol. 9(30), pp. 1-9, 2016.

[5] D. Zhou, and H. Zhang, Modified GMM background modeling and optical flow for detection of moving objects, IEEE International Conference on Systems, Man and Cybernetics, Vol. 3, pp. 2224-2229, 2005.

[6] A. K. Acharya, B. Sahoo and B. R. Swain, Object tracking using a new statistical multivariate Hotelling's T 2 approach. IEEE International Advance Computing Conference, pp. 969-972, 2014.

[7] E. Eden, D. Waisman, M. Rudzsky, H. Bitterman, V. Brod and E. Rivlin, An automated method for analysis of flow characteristics of circulating particles from in vivo video microscopy, IEEE Transactions on Medical Imaging, Vol. 24(8), pp. 1011-1024, 2005.

[8] P. Xiao, M. Duan, C. Han, S. Liu and D. Han, Maneuvering object tracking under large-area occlusive condition using mean shift embedded IMM filter. International Conference on Information, Networking and Automation, Vol. 2, p. 54, 2010. .

[9] B. B. V. L. Deepak and P. A. Singh, Survey on design and development of an unmanned aerial vehicle (quadcopter). International Journal of Intelligent Unmanned Systems, Vol. 4(2), P. 37, 2016.

[10] K. Rohr, W. J. Godinez, N. Harder, S. Wörz, J. Mattes, W. Tvaruskó and R. Eils, Tracking and quantitative analysis of dynamic movements of cells and particles. Cold Spring Harbor Protocols, Vol. 6, 2010.

[11] M. Mehta, C. Goyal, M. C. Srivastava and R. C. Jain, Real time object detection and tracking: Histogram matching and kalman filter approach. International Conference on Computer and Automation Engineering, Vol. 5, pp. 796-801, 2010.

[12] D. H. Rapoport, T. Becker, A. M. Madany, S. Schicktanz and C. Kruse, A novel validation algorithm allows for automated cell tracking and the extraction of biologically meaningful parameters. PloS one, Vol. 6(11), pp. 1-16, 2011.

[13] X Xiang, A brief review on visual tracking methods. Third Chinese Conference on Intelligent Visual Surveillance, pp. 41-44, 2011.

[14] S. K. Mohapatra, B. R. Swain, S. K. Mahapatra and S. K. Behera, Multi moving bacteria and WBC tracking using MTP approach for proper diagnosis in blood. IEEE Power, Communication and Information Technology Conference, pp. 17-21, 2015.

[15] M. M. Ata, A. S. Ashour, Y. Guo and M. M. A. Elnaby, Centroid tracking and velocity measurement of white blood cell in video. Health Information Science and Systems, Vol. 6(1), pp. 1-11, 2018.

[16] UKEssays. Real Time Video Processing and Object Detection on Android, 2018.

[17] S. Xiao and Y. Li, Visual servo feedback control of a novel large working range micro manipulation system for microassembly. Journal of Microelectromechanical Systems, Vol. 23(1), pp. 181-190, 2013.

[18] K. M. Bin Saipullah, A. Anuar, N. A. Binti Ismail and Y. Soo, Real-time video processing using native programming on Android platform. IEEE 8th International Colloquium on Signal Processing and its Applications, pp. 276-281, 2012. .

[19] W. J. B. A. Wenxing, A video supported moving object detection technique based on difference algorithm. Comput Appl Softw, Vol. 12, p. 24, 2009.

[20] X. Chen, Q. Huang, P. Hu, M. Li, Y. Tian and C. Li, Rapid and precise object detection based on color histograms and adaptive bandwidth mean shift. In 2009 IEEE/RSJ International Conference on Intelligent Robots and Systems, pp. 4281-4286, 2009.

[21] G. Lee, R. Mallipeddi, G. J. Jang and M. Lee, A genetic algorithm-based moving object detection for real-time traffic surveillance. IEEE signal processing letters, Vol. 22(10), pp. 1619-1622, 2015.

[22] H. Xu, C. Lu, R. Berendt, N. Jha and M. Mandal, Automatic nuclei detection based on generalized laplacian of gaussian filters. IEEE journal of biomedical and health informatics, Vol. 21(3), pp. 826-837, 2016.

[23] L. C. Geonzon and S. Matsukawa, Accuracy improvement of centroid coordinates and particle identification in particle tracking technique. Journal of Biorheology, Vol. 33(1), pp. 2-7, 2019.